HHS Public Access

Author manuscript

Nature. Author manuscript; available in PMC 2013 August 07.

Published in final edited form as:

Nature. 2013 February 7; 494(7435): 121–124. doi:10.1038/nature11774.

ATP-Directed Capture of Bioactive Herbal-Based Medicine on Human tRNA Synthetase

Huihao Zhou, **Litao Sun**, **Xiang-Lei Yang**, and **Paul Schimmel**

The Skaggs Institute for Chemical Biology, Department of Molecular Biology, The Scripps Research Institute, 10550 N. Torrey Pines Road, La Jolla, California, USA 92037

Febrifugine (FF) is the active component of the Chinese herb Chang Shan (*Dichroa febrifuga Lour*)[1,2], which has been used for treating malaria-induced fever for about 2000 years. Halofuginone (HF), the halogenated derivative of FF, has had clinical trials for potential therapeutic applications in cancer and fibrotic disease [3-6]. Recently, HF was reported to inhibit T_H17 cell differentiation by activating the amino acid response (AAR) pathway[7], through inhibiting human prolyl-tRNA synthetase (ProRS) to cause intracellular accumulation of uncharged tRNA[8,9]. Curiously, inhibition requires un-hydrolyzed ATP. Here we report an unusual 2.0 Å structure showing that ATP directly locks onto and orients two parts of HF onto human ProRS, so that one part of HF mimics bound proline and the other mimics the 3′-end of bound tRNA. Thus, HF is a novel ATP-dependent inhibitor that simultaneously occupies two different substrate binding sites. Moreover, our structure suggests that the efficacy of FF for malaria treatment might work by a similar mechanism. Finally, the elucidation here of a two-site modular targeting activity of HF raises the possibility that substrate-directed capture of similar inhibitors might be generalized to other synthetases.

ProRS is a member of the aminoacyl-tRNA synthetase (aaRSs) family of enzymes that activate amino acids for protein synthesis through formation of aminoacyl adenylates (AA-AMP) and subsequent transfer of the activated amino acids to the 3′-ends of the cognate tRNAs. Because of their crucial role in protein synthesis, aaRS inhibition halts the growth and suppresses viability of all cell types. Consequently, aaRSs are attractive targets for discovering drugs, like antibiotics and suppressors of cell hyperproliferation[10,11]. Many tRNA synthetase inhibitors mimic AA-AMPs, and thereby directly block the active site. Because the AA-AMP mimics occupy the active site for ATP and amino acid, they compete out the substrate ATP. In contrast, ATP was reported to be essential for HF binding to

Correspondence and requests for materials should be addressed to P.S. (schimmel@scripps.edu)..

Supplementary Information is linked to the online version of the paper at www.nature.com/nature.

Author Contributions H.Z. L.S., X.-L.Y. and P.S. designed the experiments. H.Z. and L.S. performed the experiments and all four authors analyzed the data. All authors discussed the results and H.Z. and P.S. wrote the manuscript.

Author Information Atomic coordinates and structure factors for the reported crystal structure have been deposited in the Protein Data Bank under accession code 4HVC Reprints and permissions information is available at www.nature.com/reprints.

The authors declare no competing financial interests.

Readers are welcome to comment on the online version of this article at www.nature.com/nature.

ProRS[8]. This ATP dependence suggested HF binds to ProRS through a novel mechanism and not as a mimetic of Pro-AMP. Thus, understanding how HF inhibits human ProRS is of great interest.

In its simplest description, HF is comprised of a hydroxypiperidine ring joined by bridging atoms to a double ring halogenated 4-quinazolinone (Fig. 1a). To clarify the mechanism of inhibition of HF, we cloned and expressed human ProRS and were able to obtain co-crystals with a non-hydrolyzable ATP analog ((adenosine 5′-(β,γ-imido)triphosphate)(ATP^a)) and HF, which diffracted to 2.0 Å resolution (Supplementary Table 1). The structure was solved by molecular replacement using *T. thermophilus* ProRS as template. The asymmetric unit contained two ProRS molecules that formed a homodimer (Fig. 1b), as also seen in gel filtration experiments. Each subunit encoded an N-terminal catalytic domain characteristic of a class II tRNA synthetase, an anticodon-binding domain, and a C-terminal zinc-binding domain (Fig. 1b). In the two catalytic domains of the ProRS homodimer, HF and ATP^a were bound to the active site for Pro-AMP formation (Fig. 1b, c).

ATP^a was located at the canonical ATP binding pocket of class II aaRSs[12]. Three hydrogen bonds contributed by Thr1164 and Thr1276 and hydrophobic stacking of Phe1167 stabilized the adenosine group (Supplementary Fig. 2). The ribose moiety was fixed by three hydrogen bonds with Gln1237, Thr1240 and Arg1278. The hydrogen bonds from Arg1152 and Arg1163 contributed to stabilizing the α-, β- and γ-phosphate groups of ATP^a (Supplementary Fig. 2), which form a cap over the HF binding pocket (Fig. 1c). These extensive hydrophilic and hydrophobic interactions fixed the ATP in a “U”-like bent conformation with the α-phosphate group exposed at the bottom of the U. Superposition of the catalytic domains of human ProRS with that of the previously determined structure of *T. thermophilus* ProRS showed the conformation and location of ATP was the same (Supplementary Fig. 3), with the α-phosphate group poised for proline activation. In the human ProRS:HF:ATP^a ternary complex, the α-phosphate group is proximal to the hydroxypiperidine ring of HF and forms two hydrogen bonds with its hydroxyl group (Fig. 2a, b). It also forms an additional hydrogen bond with the keto group in the bridge between the piperidine ring and the quinazolinone moiety of HF (Fig. 2a, b). These direct hydrogen-bond interactions enable ATP to lock onto and orient HF.

Beside the interactions from ATP, ProRS itself forms seven hydrogen bonds and several hydrophobic contacts with each moiety of HF (Fig. 2a, b). Thus, the pocket for the HF piperidine ring, built by Thr1121, Glu1123, Trp1169, Glu1171, His1173, Thr1240, His1242 and Ser1272 (Fig. 2c), has both hydrophobic and hydrophilic character. These residues are absolutely conserved among eukaryotic ProRS (Supplementary Fig. 4), and were found to be also important for proline recognition in the structure of *T. thermophilus* eukaryotic-like ProRS with proline (Fig. 2d)[13]. Overlay of the catalytic domains of the human and *T. thermophilus* ProRS structures showed the piperidine ring of HF bound to the same site as proline (Fig. 2e). In particular, the orientations of the proline pyrrolidine ring and of the HF piperidine ring, and the locations of nitrogen and oxygen atoms, are similar. Thus, the HF piperidine ring appears as a proline-like group, and would directly compete with proline and block proline activation. The proline mimic mechanism is consistent with HF/FF derivatives with modifications on piperidine ring being unfit for binding to the proline-binding pocket,

and, therefore, unable to inhibit or bind to ProRS or affect cell function (e.g. MAZ1310)[8]. In contrast, derivatives that replaced the piperidine ring by the pyrrolidine ring of proline retained the similar or superior biological activity that was tested[14].

The halogenated 4-quinazolinone group is buried in a pocket mainly comprised of Leu1087, Phe1097, Val1101, Pro1120, Thr1121 and Arg1152 (Fig. 2a, f). Beside the hydrogen bond between Arg1152 and nitrogen atom, the quinazolinone group was mainly stabilized by hydrophobic contacts, particularly by the hydrophobic stack effect from Phe1097 (Fig. 2a, f). ThrRS also belongs to class II aminoacyl-tRNA synthetases, and it is the closest homolog to ProRS. Arg1152 and Phe1097 of ProRS are conserved in class II synthetases. Their corresponding residues Arg363 and Tyr313 in the structure of *E. coli* threonyl-tRNA synthetase (ThrRS) were found to flank the two sides of the adenosine of A76 of $tRNA^{Thr}$ and thus play crucial roles in CCA 3′-end binding (Fig. 2g)[15]. Beside these two residues, other parts of the A76 adenosine pocket are also quite similar to the quinazolinone group binding pocket in the ProRS structure (Fig. 2g). Overlay of the ProRS and ThrRS structures by aligning the conserved 7-strand β-sheet core of their catalytic domains showed that the quinazolinone group of HF bound to the same position as bound A76, and with a similar orientation and similar side chain contacts (Fig. 2h). This structural similarity suggests that the quinazolinone group of HF binds to ProRS by employing a strategy of mimicking the terminal adenosine of the tRNA substrate. Thus, in contrast to the single-site and conventional AA-AMP mimics, HF is a dual site inhibitor by virtue of simultaneously occupying two active site pockets (Supplementary Fig. 1).

We used our crystal structure of the ProRS:ATP:HF complex to further dissect the mechanism of action of HF. Prior work by others showed that HF specifically inhibits overall aminoacylation of $tRNA^{Pro}$ and that binding of HF to ProRS is greatly enhanced by ATP[8]. (Not known was how much weaker HF binds in the absence of ATP.) According to our structure, HF is ‘two-headed’ and, with bound ATP, uses the piperidine ring to block the proline binding site and the quinazolinone group to block the site for docking the 3′-end of $tRNA^{Pro}$. We designed experiments to probe the function of each site, i.e., the site for adenylate formation/binding and that for docking the 3′-end of tRNA. In addition to HF, we used another inhibitor, Pro-SA (5′-O-(N-(L-prolyl)-sulfamoyl-adenosine), as a comparator. Pro-SA is a tight-binding non-reactive adenylate analog of Pro-AMP[16].

We first determined that the thermal melting of ProRS was barely affected by either proline or ATP[a]. In contrast, in the presence of HF, the melting curve was shifted to higher temperature by about 10 o_C by HF alone, and by about 18 o_C with HF plus ATP[a] (Fig 3a). These data show that HF binds even in the absence of ATP, and also confirm that HF binds much tighter in the presence of ATP. Not surprisingly, the thermal shift obtained with Pro-SA was the largest.

To probe the adenylate-formation site, we studied the first step of aminoacylation, which is the activation of proline by ProRS to form a tightly bound Pro-AMP adenylate complex and release of PPi.

$$ProRs+Pro+ATP \rightarrow ProRs{:}Pro-AMP+PPi$$

The conventional proline-dependent ATP-PPi exchange reaction was used. As expected, both Pro-SA and HF were potent inhibitors of this reaction in a dose-dependent fashion, with Pro-SA being more effective (Fig. 3b). This result is consistent with the thermal melting data of Figure 3a showing the tighter binding of Pro-SA, and with our x-ray crystal structure showing the docking of one 'head' of HF at the site for the prolyl moiety of Pro-AMP.

Next, we investigated the ability of HF to mimic docking of A76 of $tRNA^{Pro}$ to ProRS. For this purpose we studied the effect of HF on the relatively stable preformed ProRS:Pro-AMP complex, which was isolated on a column. Because binding of tRNA to tRNA synthetases is generally associated with conformational changes that mobilize the active site for transfer of the activated amino acid to A76, we reasoned that binding of the A76-mimicking quinazolinone group of HF would result in an abortive transfer and thereby release Pro-AMP from ProRS. Accordingly, the ProRS:Pro-AMP complex was incubated separately with Pro-SA (which should not have access to the A76 site) and with HF (without ATP). As expected, Pro-SA caused some reduction in the bound Pro-AMP, which is attributed to an exchange on the enzyme between bound Pro-AMP and Pro-SA. In contrast, free HF, while having a much lower affinity than Pro-SA for ProRS, completely released Pro-AMP from the complex (Fig. 3c).This result supports the conclusion (from our x-ray structure) that HF also mimics A76 of tRNA.

HF is a halogenated derivative of febrifugine, which is the bioactive constituent in the Chang Shan herb that has long been used to treat malaria. The human and malaria parasite *P. falciparum* ProRS binding sites are highly conversed (Supplementary Fig. 4). With that in mind, using our ATP-dependent docking of HF to human ProRS as a template, we were able to show the potential for docking of FF to *P. falcipaurm* ProRS (Fig. 4). Thus, our analysis suggests malarial ProRS may also be the target of FF. This possibility could also explain why the killing effect of FF on *P. falciparum* in culture is reversed by proline[8].

Interestingly, in addition to the inhibition of amino acid activation by mimics of AA-AMP (including the "operational" mimic pseudomonic acid (mupirocin)[17]), the ATP-dependent two-site HF inhibition mechanism reported here, and the single-site tRNA-dependent editing-site-trapping mechanism reported earlier[18], illustrate two entirely different and unusual mechanisms for substrate participation in capture of an inhibitor (Supplementary Fig. 5). In addition, by substitution of the piperidine ring with other amino acid mimics, dual site inhibitors could in principle be designed for some other aaRSs.

METHODS

Protein expression and purification

The cDNA fragment encoding human prolyl-tRNA synthetase (ProRS) was cloned into *E.coli* plasmid pET21a (Novagen, Darmstadt, Germany), with an additional N-terminal His6-tag. The plasmid encoding ProRS was transformed into *E.coli* strain BL21(DE3) pLysS (Life Technologies, San Diego, CA) and was induced overnight for overexpression with 0.5 mM IPTG at room temperature. The *E.coli* cell lysate was firstly loaded onto a Ni-NTA column (Qiagen, Valencia, CA), and the elution fraction was further purified with

mono Q ion-exchange chromatography (GE Healthcare, 5/50 GL, Piscataway, NJ) to a single band as indicated on SDS-PAGE with Coomassie brilliant blue staining. The purified protein was found as a single peak with the elution volume consistent with a homogeneous ProRS homodimer on the Superdex 200 analytical gel filtration column (GE Healthcare, 10/300 GL). The purified ProRS was finally concentrated to 50 mg/mL and stored at −80°C in a buffer of 50 mM NaCl, 2 mM Tris (pH 8.0).

Crystallization and data collection

ProRS was crystallized with the sitting-drop vapor-diffusion method using a Mosquito robot (TTP Labtech, Cambridge, MA). Prior to crystallization, ProRS was diluted to 40 mg/mL with 3 mM halofuginone (racemic mixture) (Sigma-Aldrich, Saint Louis, MO), 5 mM ATP analog adenosine 5′-(β,γ-imido)triphosphate (Sigma-Aldrich), 5 mM $MgCl_2$ and 5 mM β-mercaptoethanol, and then incubated on ice for 30 min. Next, sitting drops were set up by mixing 100 nL of protein (40 mg/mL) and 100 nL of reservoir solution containing 20% (*w*/*v*) PEG 3350, 0.6 M $CaCl_2$ and 50 mM HEPES (pH 7.5), and equilibrated against a 70 μL of reservoir solution at 30°C for 2–3 days before data collection. The X-ray diffraction data were collected using a single crystal at a wavelength of 1.000 Å and temperature of 100 o_K at beamline 7-1 of Stanford Synchrotron Radiation Lightsource (SSRL). The complete data set contains 500 images with the oscillation angle of 0.5° for each image. The ProRS:HF:ATP[a] crystal belonged to space group $P2_1$. Data were integrated and scaled with the program HKL2000[22].

Structure determination and refinement

The initial model was determined by molecular replacement using the program MOLREP[23]. The crystal structure of *T. thermophilus* ProRS (PDB code 1HC7), which has 43% sequence identity to human ProRS, was used as the searching model. The structure was further refined by iterative cycles of positional refinement and TLS refinement with Refmac5[24] and Phenix[25] and model building with COOT[26], and the final model was refined to 2.0 Å resolution with R_{work}/R_{free} of 20.4%/22.7%. The model has good geometry quality, and 98.9%/99.8% residues are in favored/allowed regions of the MolProbity[27] Ramachandran plot. Statistics of data collection and structure refinement are given in Supplementary Table 1. The atomic coordinates and structural factors have been deposited into Protein Data Bank under the code 4HVC.

Sequence analysis and Structure Presentation

Protein sequences were aligned using the program Multalin[28]. The alignment result was submitted to ESPript[29] for figure generation. All protein structure illustrations were prepared with the program PyMol (www.pymol.org).

Thermal Shift Assay

ProRS (3 μg) was diluted in 30 μL buffer containing 500 mM NaCl, 20 mM Tris pH 8.0, 1/2500 SYPRO Orange dye (Life Technologies) and different ligands (5 mM ATP[a], 5 mM proline, 1 mM HF, 1 mM HF + 5 mM ATP[a], or 1 mM Pro-SA, respectively), and incubated at room temperature for 10 min. Then, ProRS samples were heated from 25 to 98°C at a rate

of 1°C/min, and the fluorescence signals were monitored by the StepOnePlus real-time PCR system (Life Technologies). Each curve is an average of three measurements.

ATP-pyrophosphate exchange assays

The reaction buffer contained 100 mM HEPES pH 7.5, 20 mM KCl, 10 mM $MgCl_2$, 1 mM DTT, 2 mM ATP, 1 mM Na pyrophosphate (NaPPi), 20 μCi/ml ^{32}P-PP_i and 0.5 mM proline. Inhibitor HF and Pro-SA (5′-*O*-(*N*-(L-prolyl)-sulfamoyl)adenosine (kindly provided by Prof. Karin Musier-Forsyth, The Ohio State University) were added at different concentrations (0, 30 or 90 nM). The reactions were started by adding ProRS into buffer at the final concentration of 10 nM, and then incubated at 20°C. 20 μL of each of the reactions was quenched at different time points in 200 μL quench buffer (1 M HCl, 200 mM NaPPi, 4% charcoal). The free ^{32}P-PP_i was removed by flowing through the 96-well PVDF filter plates, and the residual ^{32}P-PP_i was washed five times using 200 μL washing buffer (1 M HCl and 200 mM NaPPi). Then, the produced ^{32}P-ATP remaining in filter plates was transferred to scintillation vials and counted. The data were analyzed with GraphPad Prism (GraphPad Software, La Jolla, CA). The experiments here and below were independently repeated three times with duplicated measurements each time.

HF - Pro-AMP competition assay

The isolation of ProRS:Pro-AMP was slightly modified from that of a previous report[30]. In brief, 2 μM ProRS was added to the buffer containing 50 mM HEPES (pH 7.5), 20 mM KCl, 5 mM $MgCl_2$, 2 mM ATP, 2 mM DTT, 20 μM proline and 1 μM ^{3}H-proline, and then incubated at 4°C for 10 min to create ProRS:^{3}H-Pro-AMP. The reaction containing ProRS:^{3}H-Pro-AMP was flowed through a desalting column (SpinTrap G-25, GE healthcare) to isolate the complex and remove the extra ATP and proline. HF and Pro-SA were added at the concentration of 4 μM to the complex to compete for 10 min at 20°C. The reaction was passed through desalting column again to remove dissociated ^{3}H-Pro-AMP. The eluted ^{3}H-Pro-AMP still bound to ProRS was then measured.

Supplementary Material

Refer to Web version on PubMed Central for supplementary material.

Acknowledgement

We thank Prof. Karin Musier-Forsyth (The Ohio State University) for providing the ProRS gene and Pro-SA, staff at beamline 7-1 of Stanford Synchrotron Radiation Lightsource (SSRL) for assistance in X-ray diffraction data collection, and Prof. Min Guo (The Florida Scripps Research Institute) for comments. This work was supported by grants GM15539, 23562 and 88278 from the NIH and by a fellowship from the National Foundation for Cancer Research.

REFERENCES

1. Koepfli JB, Mead JF, Brockman JA Jr. An alkaloid with high antimalarial activity from Dichroa febrifuga. J. Am. Chem. Soc. 1947; 69:1837. [PubMed: 20251439]
2. Coatney GR, Cooper WC, Culwell WB, White WC, Imboden CA Jr. Studies in human malaria. XXV. Trial of febrifugine, an alkaloid obtained from Dichroa febrifuga lour., against the Chesson strain of Plasmodium vivax. J. Natl. Malar. Soc. 1950; 9:183–6. [PubMed: 15422372]

3. Pines M, Snyder D, Yarkoni S, Nagler A. Halofuginone to treat fibrosis in chronic graft-versus-host disease and scleroderma. Biol. Blood. Marrow Transplant. 2003; 9:417–25. [PubMed: 12869955]
4. Pines M, Nagler A. Halofuginone: a novel antifibrotic therapy. Gen. Pharmacol. 1998; 30:445–50. [PubMed: 9522159]
5. de Jonge MJ, et al. Phase I and pharmacokinetic study of halofuginone, an oral quinazolinone derivative in patients with advanced solid tumours. Eur. J. Cancer. 2006; 42:1768–74. [PubMed: 16815702]
6. Koon HB, et al. Phase II AIDS Malignancy Consortium trial of topical halofuginone in AIDS-related Kaposi sarcoma. J. Acquir. Immune. Defic. Syndr. 2011; 56:64–8. [PubMed: 21068672]
7. Sundrud MS, et al. Halofuginone inhibits TH17 cell differentiation by activating the amino acid starvation response. Science. 2009; 324:1334–8. [PubMed: 19498172]
8. Keller TL, et al. Halofuginone and other febrifugine derivatives inhibit prolyl-tRNA synthetase. Nat. Chem. Biol. 2012; 8:311–7. [PubMed: 22327401]
9. Kilberg MS, Pan YX, Chen H, Leung-Pineda V. Nutritional control of gene expression: how mammalian cells respond to amino acid limitation. Annu. Rev. Nutr. 2005; 25:59–85. [PubMed: 16011459]
10. Schimmel P, Tao J, Hill J. Aminoacyl tRNA synthetases as targets for new anti-infectives. FASEB J. 1998; 12:1599–609. [PubMed: 9837850]
11. Hill, J. Aminoacyl sulfamides for the treatment of hyperproliferative disorders Cubist Pharmaceuticals, Inc. U.S. Patent. 5,824,657. 1998.
12. Carter CW Jr. Cognition, mechanism, and evolutionary relationships in aminoacyl-tRNA synthetases. Annu. Rev. Biochem. 1993; 62:715–48. [PubMed: 8352600]
13. Yaremchuk A, Tukalo M, Grotli M, Cusack S. A succession of substrate induced conformational changes ensures the amino acid specificity of Thermus thermophilus prolyl-tRNA synthetase: comparison with histidyl-tRNA synthetase. J. Mol. Biol. 2001; 309:989–1002. [PubMed: 11399074]
14. Zhu S, et al. Synthesis and biological evaluation of febrifugine analogues as potential antimalarial agents. Bioorg. Med. Chem. 2009; 17:4496–502. [PubMed: 19467876]
15. Sankaranarayanan R, et al. The structure of threonyl-tRNA synthetase-tRNA(Thr) complex enlightens its repressor activity and reveals an essential zinc ion in the active site. Cell. 1999; 97:371–81. [PubMed: 10319817]
16. Heacock D, Forsyth CJ, Shiba K, Musier-Forsyth K. Synthesis and aminoacyl-tRNA synthetase inhibitory activity of prolyl adenylate analogs. Bioorg. Chem. 1996; 24:273–89.
17. Nakama T, Nureki O, Yokoyama S. Structural basis for the recognition of isoleucyl-adenylate and an antibiotic, mupirocin, by isoleucyl-tRNA synthetase. J. Biol. Chem. 2001; 276:47387–93. [PubMed: 11584022]
18. Rock FL, et al. An antifungal agent inhibits an aminoacyl-tRNA synthetase by trapping tRNA in the editing site. Science. 2007; 316:1759–61. [PubMed: 17588934]
19. Pantoliano MW, et al. High-density miniaturized thermal shift assays as general strategy for drug discovery. J. Biomol. Screen. 2001; 6:429–40. [PubMed: 11788061]
20. Arnold K, Bordoli L, Kopp J, Schwede T. The SWISS-MODEL workspace: a web-based environment for protein structure homology modeling. Bioinformatics. 2006; 22:195–201. [PubMed: 16301204]
21. Beebe K, et al. A universal plate format for increased throughput of assays that monitor multiple aminoacyl transfer RNA synthetase activities. Anal. Biochem. 2007; 368:111–21. [PubMed: 17603003]
22. Otwinowski Z, Minor W. Processing of X-ray diffraction data collected in oscillation mode. Methods in Enzymology. 1997; 276:307–26.
23. Vagin A, Teplyakov A. MOLREP: an Automated Program for Molecular Replacement. J. Appl. Cryst. 1997; 30:1022–25.
24. Murshudov GN, Vagin AA, Dodson EJ. Refinement of macromolecular structures by the maximum-likelihood method. Acta. Crystallogr. D. Biol. Crystallogr. 1997; 53:240–55. [PubMed: 15299926]

25. Adams PD, et al. PHENIX: a comprehensive Python-based system for macromolecular structure solution. Acta. Crystallogr. D. Biol. Crystallogr. 2010; 66:213–21. [PubMed: 20124702]
26. Emsley P, Cowtan K. Coot: model-building tools for molecular graphics. Acta. Crystallogr. D. Biol. Crystallogr. 2004; 60:2126–32. [PubMed: 15572765]
27. Chen VB, et al. MolProbity: all-atom structure validation for macromolecular crystallography. Acta. Crystallogr. D. Biol. Crystallogr. 2010; 66:12–21. [PubMed: 20057044]
28. Corpet F. Multiple sequence alignment with hierarchical clustering. Nucleic Acids Res. 1988; 16:10881–90. [PubMed: 2849754]
29. Gouet P, Courcelle E, Stuart DI, Metoz F. ESPript: analysis of multiple sequence alignments in PostScript. Bioinformatics. 1999; 15:305–8. [PubMed: 10320398]
30. Shi JP, Schimmel P. Aminoacylation of alanine minihelices. “Discriminator” base modulates transition state of single turnover reaction. J. Biol. Chem. 1991; 266:2705–8. [PubMed: 1704363]

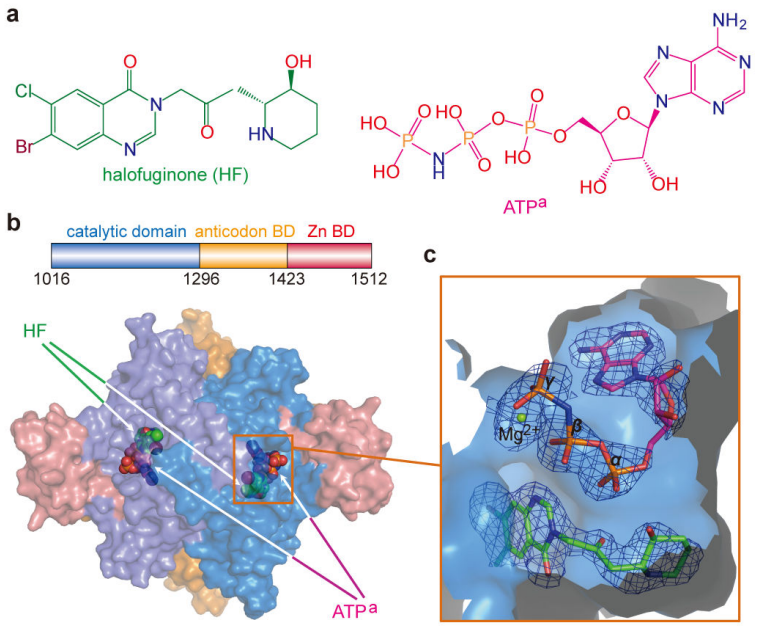

Figure 1. Structure of human ProRS and of bound ligands

a, Chemical structures of halofuginone (HF) and the ATP analog (ATP^a). **b**, Two ProRS monomers form an asymmetric unit that is a homodimer. HF and ATP^a are shown as spherical models at the active site of both subunits. Here and throughout, ATP^a and HF are colored as in Fig.1a. **c**, HF is buried at the bottom of the pocket and covered by co-bound ATP^a. A simulated annealing omit map was calculated with Fourier coefficients $2F_o$-F_c, and contoured at 1.5σ.

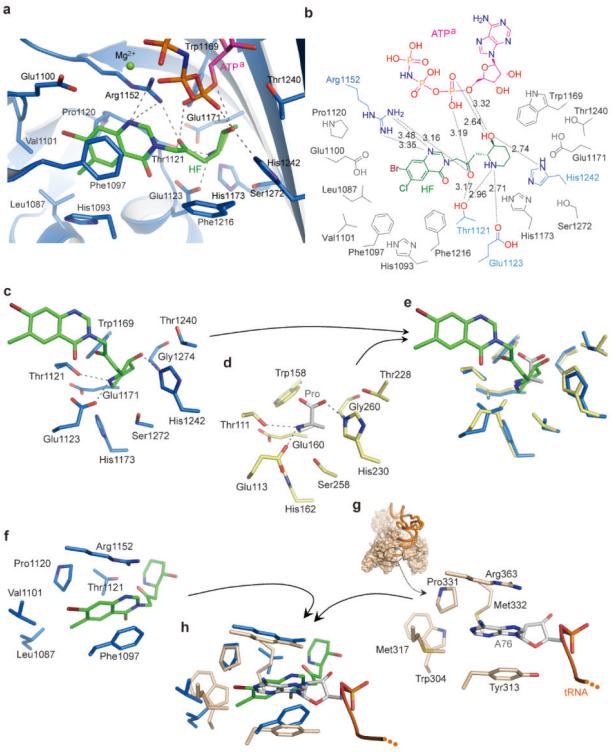

Figure 2. Mechanistic basis for ATP-dependent inhibition of ProRS by halofuginone

a, HF forms extensive hydrophobic contacts and hydrogen-bonding interactions with ProRS and with ATP[a]. **b**, Two-dimensional presentation of HF binding. The HF, ATP[a] and hydrogen-bonded residues are colored as previously, and other residues within 4 Å of HF are colored in gray. **c**, A stick model showing the binding of HF's piperidine ring to human ProRS. **d**, The proline binding pocket of *T. thermophilus* ProRS in complex with proline (PDB 1H4T, protein is colored as yellow and proline as gray-white). **e**, Structure superposition of catalytic domain of human ProRS with *T. thermophilus* ProRS reveals the piperidine ring of HF directly occupies the proline binding pocket. **f**, The stick model showing the binding of the halogenated 4-quinazolinone group of HF to human ProRS. **g**, Structure of *E. coli* ThrRS:tRNA complex, with the pocket for the adenosine group for A76 (PDB 1QF6). **h**, Overlay of the catalytic domain of human ProRS onto *E. coli* ThrRS (brown) reveals that HF uses the binding pocket for A76 of the CCA^{76}-3′ end for binding the quinazolinone moiety.

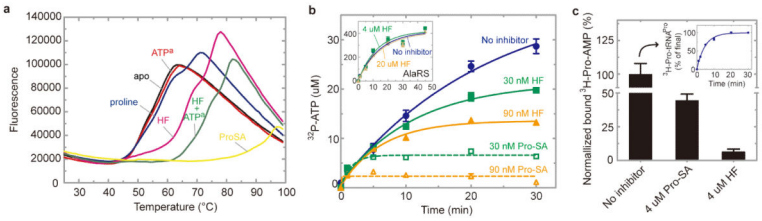

Figure 3. HF interacts with both the site for amino acid activation and the site for docking the 3′-end of tRNA

a, Thermal melting[19] of ProRS in the presence of different ligands. HF binds in the absence of ATP^a, and binds more strongly in the presence of ATP^a. **b**, HF and the comparator Pro-SA block formation of Pro-AMP, in the proline-dependent ATP-PPi exchange reaction. The inset shows that HF had no effect on the alanine-dependent ATP-PPi exchange reaction with AlaRS. **c**, HF mobilizes the release of Pro-AMP from ProRS. The ProRS:^{3}H-Pro-AMP complex was prepared on ice and then isolated on a column and for 10 min was left untreated, or exposed to HF, or exposed to Pro-SA, respectively. The complex was then re-run on the column and the amount of bound ^{3}H-Pro-AMP was determined. The inset shows that the isolated ^{3}H-Pro was activated (as ^{3}H-Pro-AMP) and could be transferred to tRNA. Error bars are s.e.m. (n=2).

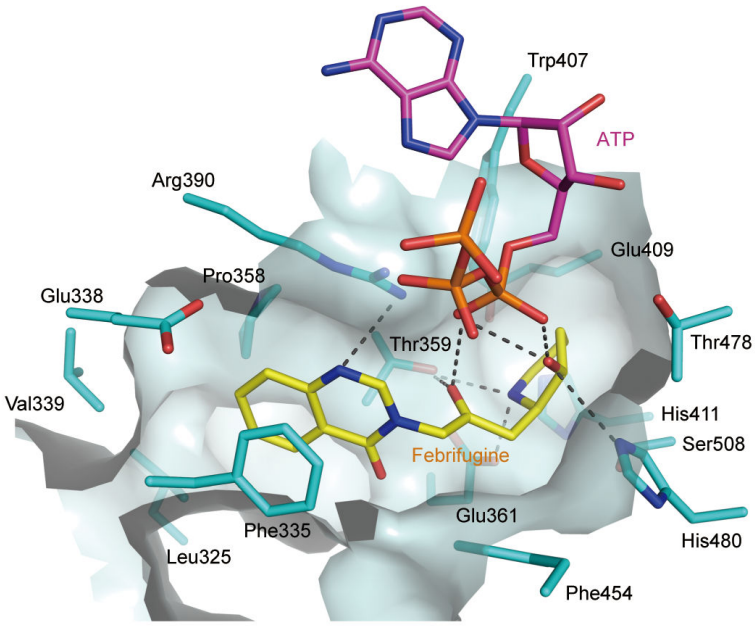

Figure 4. FF blocks ProRS

Febrifugine (FF) docked to the active site of *P. falcipaurm* ProRS (UniProtKB code Q8I5R7). ProRS and FF are colored as cyan and yellow, respectively. The hydrogen bonds are indicated with dashes. The *P. falciparum* ProRS structure was generated by the protein structure homology-modeling sever SWISS-MODEL[20]. FF was docked into the *P. falciparum* ProRS active site based on the structure of ProRS:halofuginone:ATP[a] complex, while ATP was docked based on the structure of the *T. thermophilus* ProRS:tRNA:ATP complex (PDB code 1H4Q).